RECENT MODEL RESULTS ON NLC AND PMSE FORMATION

Markus Rapp and Franz-Josef Lübken

Leibniz-Institute of Atmospheric Physics, 18225 Kühlungsborn, Germany

ABSTRACT

We describe a model of electron diffusion in the vicinity of charged aerosols in order to explain the reduction of electron mobility needed for the existence of PMSE. The physical processes involved are introduced and the model is used to explain recent observations of an artificial modulation of PMSE by ionospheric heating with the EISCAT heating facility. Using then a microphysical model of the generation and growth of mesospheric ice particles we consider whether the model yields a large enough number of negatively charged ice particles needed to understand the electron diffusivity reduction in terms of the physical processes currently incorporated in the ice particle model. Then introducing the charge number density of aerosol particles times the mean aerosol radius squared as a proxy for the possible existence of PMSE we find a nice agreement of simulated altitude profiles and the mean height distribution of PMSE. Finally, we find that at the lower edge of the ice particle layer the particles have grown large enough in order to give rise to an optically observable signal recognized as NLC. Thus our model calculations yield PMSE in an altitude range from roughly 81–90 km with the NLC located at the lower edge. This pattern is consistent with the majority of common volume observations of NLC and PMSE.

1. INTRODUCTION

Noctilucent clouds (NLC) and polar mesosphere summer echoes (PMSE) are intriguing phenomena which are observed in the vicinity of the cold polar summer mesopause region. There is now firm evidence that NLC are due to sunlight scattering from ice particles at altitudes roughly around 83 km with typical radii of 20–50 nm and number densities of $\sim$100 cm^{-3} [*von Cossart et al.*, 1999; *Hervig et al.*, 2001]. PMSE on the other hand are extremely strong radar echoes from the same altitude region and were first discovered in the VHF band [*Czechowsky et al.*, 1979; *Ecklund and Balsley*, 1981] at frequencies of 50 MHz corresponding to a wavelength of 6 m. The echoes are believed to be at least partly caused by the existence of a large number of small ice particles with typical radii and number densities of 10 nm and $\sim$ 1000 cm^{-3}, respectively. These small ice particles capture electrons and positive ions from the background plasma of the D-region and thus acquire typically one net negative elementary charge because of the much higher mobility of electrons compared to positive ions [e. g., *Rapp and Lübken*, 2001]. Due to the multipolar electric fields between electrons, positive ions and negatively charged aerosols the diffusivity of the electrons is effectively reduced. Thus fluctuations in electron density which determine the radar refractive index on spatial scales as small as the half radar wavelength can persist in spite of the influence of viscous forces which tend to smooth out gradients on such small spatial scales [*Kelley et al.*, 1987; *Cho et al.*, 1992]. This idea is supported by recent observations of *Chilson et al.* [2000] who reported about an artificially induced modulation of PMSE when the electrons at PMSE altitudes were heated to temperatures of about 3000 K with the EISCAT heating facility [*Belova et al.*, 2001]. The PMSE disappeared within a few seconds when the heater was switched on and reappeared within a few seconds when the heater was switched off again. *Rapp and Lübken* [2000] applied a model of electron diffusion in the vicinity of charged aerosols to this problem and could both reproduce the instantaneous fade out of the PMSE signal as well as the recovery when the electron temperature relaxed back to the ambient temperature of the neutral atmosphere.

In this paper we present a detailed description of the electron diffusion model applied by *Rapp and Lübken* [2000]. Using this model we give some insight into the physical processes leading to the reduction of electron diffusivity due to the presence of charged aerosol particles in the 'normal' case that electrons and neutrals are in thermal equilibrium. Then we shortly summarize the influence of enhanced electron temperatures on the electron diffusion time constants. In the second part of this paper we then focus on the point whether the existence of the aerosol particles can be understood employing a microphysical model of the nucleation and development of ice particles in the polar summer mesopause region which give rise to NLC and PMSE. Finally we present some new ideas how these calculated ice particle parameters can be related to the characteristics of PMSE.

Proceedings of the 15th ESA Symposium on European Rocket and Balloon Programmes and Related Research, Biarritz, France, 28 31 May 2001 (ESA SP-471, August 2001)

2. ELECTRON DIFFUSION

The formulation of our multiconstituent plasma diffusion model closely follows the work of *Hill* [1978]. Hill has treated the case of equal temperatures of all plasma constituents which is reasonable in the D region where the high collision frequency with the neutral gas provides thermal equilibrium of all constituents. To describe the diffusion of a multiconstituent plasma we assume quasi neutrality, i. e., that the inhomogeneities under consideration are significantly larger than the electron Debye length. The electron Debye length, r_D, is given by

$$r_D = \sqrt{\frac{\epsilon_0 k T_e}{n_e e^2}} \tag{1}$$

with the dielectric constant ϵ_0, Boltzmann's constant k, the electron temperature T_e, the elementary charge e, and the electron number density n_e. Using a reasonable electron number density of 1000 cm^{-3} at 85 km altitude we thus obtain r_D=2.5 cm for an undisturbed temperature of 150 K and 11.9 cm for 3000 K as appropriate for heating conditions [*Belova et al.*, 2001], respectively. Both values are much smaller than the spatial inhomogeneities under consideration, i. e., the half radar wavelength of the EISCAT VHF radar (67 cm). We further take the neutral gas to be at rest, and neglect possible external electric and magnetic fields. Then the equation of motion of the charged species is given by

$$n_j q_j \vec{E} = \nabla p_j + m_j \nu_j \vec{\Gamma}_j \tag{2}$$

where n_j is the number density, q_j the charge, p_j the partial pressure, m_j the mass, ν_j the collision frequency with the neutral gas, and $\vec{\Gamma}_j$ the flux of the j-th plasma constituent. The partial pressure p_j can be expressed as $p_j=n_j k T_j$. The multipolar electric field is given by Maxwell's law, i. e.,

$$\nabla \vec{E} = 4\pi \sum_j q_j n_j \tag{3}$$

It is further useful to introduce the diffusion coefficient $D_j=kT_j/(m_j\nu_j)$ and the mobility $\mu_j=q_j/(m_j\nu_j)$. With these definitions equation 2 can be written as

$$n_j \mu_j \vec{E} = D_j \nabla n_j + \vec{\Gamma}_j \tag{4}$$

If we now multiply equation 4 with q_j, sum over all j and assume that $\sum_j q_j \vec{\Gamma}_j = 0$ (quasi neutrality) the multipolar electric field can be expressed as

$$\vec{E} = \frac{\sum_j q_j D_j \nabla n_j}{\sum_j q_j n_j \mu_j} \tag{5}$$

In order to give an estimate of the magnitude of this multipolar electric field we approximate equation 5 by its contributions by electrons which is reasonable because $D_e \gg D_{j\neq e}$ and $\mu_e \gg \mu_{j\neq e}$. If we further use the definitions of D_e and μ_e we obtain:

$$\vec{E} = -\frac{kT_e}{e}\frac{1}{n_e}\nabla n_e \tag{6}$$

Using a relative electron density fluctuation of $\Delta n_e/n_e$=0.1 [e. g., *Blix and Thrane*, 1993] and Δx=1 m appropriate for PMSE we obtain an electric field of $\approx$ 2 mV/m for a typical temperature of 150 K.

We now use expression 5 in equation 4 to determine an expression for the fluxes Γ_j. Using further the condition for charge neutrality, i. e., $\sum_j q_j n_j = 0 \Leftrightarrow \sum_j q_j \nabla n_j = 0$, and again that $D_e \gg D_{j\neq e}$ and $\mu_e \gg \mu_{j\neq e}$ we finally obtain:

$$\Gamma_{j\neq e} = -D_j \nabla n_j + n_j \frac{q_j}{q_e}\frac{T_e}{T_j} D_j \frac{\sum_{k\neq e} q_k \nabla n_k}{\sum_{k\neq e} q_k n_k} \tag{7}$$

We now consider a plasma consisting of electrons, one group of positive ions with number density n_i and one group of singly negatively charged aerosol particles with number density N_A. In general the continuity equation of each of these species can be written as

$$\frac{\partial n_j}{\partial t} + \nabla \vec{\Gamma}_j = 0 \tag{8}$$

Quasi neutrality requires that $n_e=n_i-N_A$, and $\vec{\Gamma}_e=\vec{\Gamma}_i-\vec{\Gamma}_A$. For algebraical convenience we further introduce the quantity $n_\oplus = n_i + N_A$, i.e. the total number density of plasma species different from electrons. The use of equations 7 and 8 then leads to the two following continuity equations for n_e and $n_\oplus$ (n_i and N_A can be derived from these two quantities by means of $n_i=(n_\oplus+n_e)/2$ and $N_A=(n_\oplus - n_e)/2$, respectively):

$$\frac{\partial n_e}{\partial t} = \frac{D_i - D_A}{2}\Delta n_\oplus + \left[\frac{T_e}{T_i}D_i + \frac{D_i + D_A}{2}(1 + 2\Lambda\frac{T_e}{T_i})\right]\Delta n_e \tag{9}$$

$$\frac{\partial n_\oplus}{\partial t} = \frac{D_i + D_A}{2}\Delta n_\oplus + \left[\frac{T_e}{T_i}D_i + \frac{D_i - D_A}{2}(1 + 2\Lambda\frac{T_e}{T_i})\right]\Delta n_e \tag{10}$$

where D_i and D_A are the diffusion coefficients of positive ions and negatively charged aerosols, respectively and Λ is defined as $\Lambda = N_A/n_e$. Following *Cho et al.* [1992] these quantities can be expressed as follows:

$$D_i = \frac{3kT}{16\mu_{in} n_n \Omega_{in}} \tag{11}$$

$$D_A = 4.14 \cdot 10^{-7}\sqrt{\frac{e^2\gamma\mu_{in}}{2\epsilon_0 kT m_n}} \cdot \frac{D_i}{r_A^2} \tag{12}$$

where μ_{in} is the reduced mass of a positive ion and a neutral air molecule, n_n the neutral air number density, and Ω_{in} the collision integral as determined from the polarization interaction model. γ is the neutral atom polarizability, m_n the mass of an air molecule, and r_A the radius of the aerosol particle. Typical values for D_i and D_A are 0.4 m^2/s and 0.0017 m^2/s

(r_A=10 nm), respectively, if we assume positive ions of mass 91 amu ($H^+(H_2O)_5$) which is a dominant ion species at 85 km altitude [*Kopp et al.*, 1985].

We now proceed discussing the influence of negatively charged aerosol particles on an idealized disturbance in the plasma densities relative to an smooth background profile in the case that T_e=T_i=T_n where T_n is the neutral temperature. We consider the temporal evolution of a disturbance in the electron profile with an initial Gaussian shape, i. e. $n_e(x, t=0) = n_e(0,0) \cdot \exp(-x^2/2\sigma^2)$. Charge neutrality requires $n_\oplus(x,0) = n_e(x,0) \cdot (1+2\Lambda)$.
In Figure 1 we present electron, positive ion, and negatively charged aerosol distributions calculated by a numerical integration of equations 9 and 10 for different times of diffusion in a case where most of the negative charge is bound to the aerosols (Λ =5). This is appropriate e.g. in altitude regimes where deep electron biteouts occur [*Lübken et al.*, 1998]. From Figure 1 we see that the aerosol particle disturbance merely changes for the considered time scales due to their low mobility. By Coulomb repulsion they thus force a negative disturbance in the electron density profile to develop. This negative disturbance can only decay with the time constant of the decay of the aerosol disturbance. In other words the diffusion time constant of electrons is shifted towards the diffusion time constant of the charged aerosols, thus varying like $1/r_A^2$ (see equation 12).
It is interesting to note that the above mentioned reduction of electron diffusivity can also be derived analytically. *Hill* [1978] considered the solution of equations 9 and 10 for the intial conditions stated above. According to his analysis the solution for the electron density can be written as:

$$\frac{n_e(x,t)}{n_e(0,0)} = A_2 \cdot H(D_1^0, x, t) - A_1 \cdot H(D_2^0, x, t) \quad (13)$$

with

$$H(D,x,t) = \frac{1}{\sqrt{1+2Dt/\sigma^2}} \cdot \exp\left(-\frac{x^2/\sigma^2)}{2(1+2Dt/\sigma^2)}\right) \quad (14)$$

$$D_{1/2}^0 = \frac{1}{2}[D_i + (D_i + D_A)(1+\Lambda)] \pm$$

$$\frac{1}{2}\sqrt{D_i^2(\Lambda+2)^2 + 2D_iD_A(\Lambda-2)(\Lambda+1) + D_A^2(\Lambda+1)^2} \quad (15)$$

$$A_q = \frac{2D_i(1+\Lambda) - D_q^0}{D_1^0 - D_2^0} \quad (16)$$

Note that the quantities $D_{1,2}^0$ have a direct physical meaning: they are the diffusion coefficients appropriate for the two diffusion modes of the system because there is an electric field both between electrons and charged aerosol particles as well as between electrons and positive ions. From Figure 1 it is evident that it is the decay time of the negative electron disturbance due to the aerosol disturbance which determines the overall decay time of the electron disturbance because this negative disturbance can only decay when

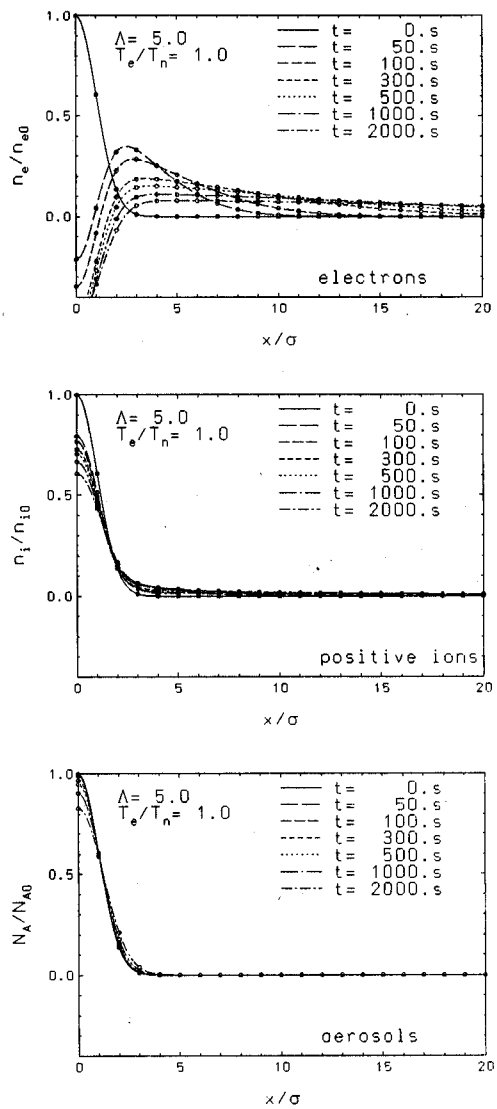

Figure 1. Electron, positive ion, and negatively charged aerosol distributions for different times of diffusion in a case that most of the negative charge is bound to the aerosols, i.e. $\Lambda = N_A/ne$=5.

the aerosol disturbance decays. To investigate the influence of charged aerosols on the decay time of the system we can thus investigate the temporal evolution of $n_e(x=0,t)$ for different values of Λ. The result of this calculation for an electron disturbance with σ=3 m is presented in Figure 2. Defining the electron decay time τ as the time when the disturbance becomes smaller than 10% of its initial value for all times larger than τ we see that there is a dramatic variation of τ with Λ: While in the absence of charged aerosols ($\Lambda = 0$) τ=5min, for Λ =0.9 it is already 2.5 hours, and asymptotically reaches a value of ~15 hours for $\Lambda \to \infty$.

We now turn to the problem of heating: In Figure 3 we present the temporal evolution of electron disturbances similar to the ones presented in Figure 1, however, this time for different electron temperatures, i. e., T_e/T_n=5 and 20. As is clearly seen from Figure 3 the electron disturbance decays faster the more the

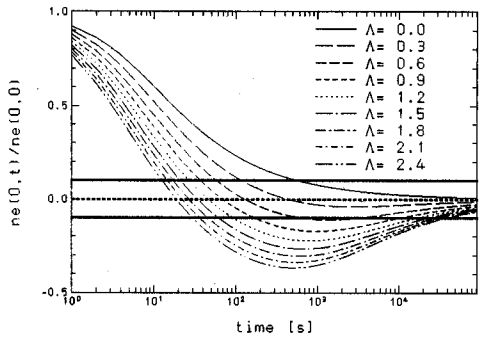

Figure 2. Analytical results of the decay of a Gaussian disturbance with σ=3m in the electron density profile for different values of the parameter $\Lambda = N_a/n_e$.

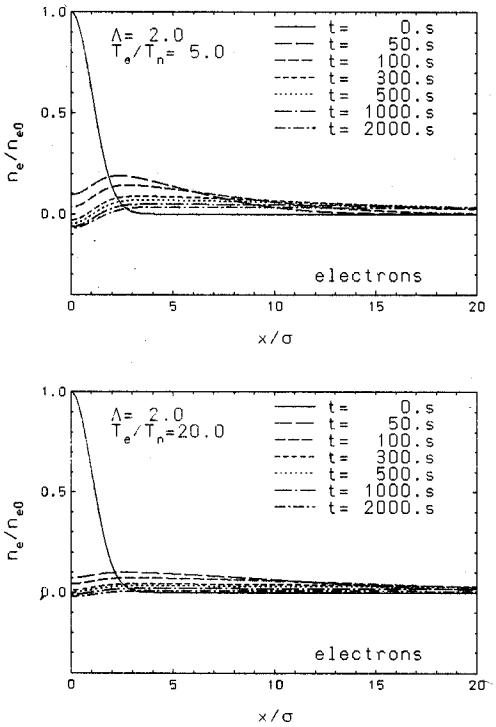

Figure 3. Decay of electron density disturbances in the presence of negatively charged aerosol particles for different electron temperatures.

electron temperature is enhanced. The physical reason for this fact is directly evident from equation 6: as the ambipolar electric field is directly proportional to the electron temperature the force acting on the electrons to smooth out any gradient also increases like T_e and thus the electron density disturbance quickly disappears. Considering here spatial scales appropriate for the EISCAT VHF radar ($\lambda/2$=67cm) *Rapp and Lübken* [2000] have calculated that the decay time reduces to less than 1 s thus nicely explaining the experimental results of *Chilson et al.* [2000]. More than that, *Rapp and Lübken* [2000] could also explain the fast recovery of the PMSE when the heater was switched off: The disturbance in the aerosol density profile is not at all affected by the increased electron temperature. Thus as soon as the electrons have thermalized the Coulomb repulsion due to the charged particles immediately acts on the electrons and forces them 'back' into their position before the heating pulse.

3. MODEL SIMULATIONS OF ICE PARTICLE GROWTH IN THE MESOPAUSE REGION

In this section we now turn to the question whether the presence of ice particles needed for the above described mechanism can be explained in terms of a microphysical model of the nucleation, growth, and development of mesospheric aerosol particles.

3.1. Ice particle evolution

We apply the CARMA model which is a successor version of the microphysical models of *Turco et al.* [1982] and *Jensen and Thomas* [1988]. Recently this model has been revived in order to interpret rocket-borne observations of small scale temperature structures in the vicinity of NLC [*Rapp et al.*, 2001]. Details of the model can also be found in the above mentioned references.

We have run the model assuming a background temperature profile for the 1st of July as given in *Lübken* [1999] and a water vapor mixing ratio profile from *Körner and Sonnemann* [2001]. Based on the observations of *Rapp et al.* [2001] we have also superimposed gravity wave disturbances on the mean temperature profile leading to a temporarily stronger NLC brightness compared to an undisturbed atmosphere. One day averages of the ice number densities and mean radii calculated with the model are presented in Figure 4. In addition we have indicated the average backscatter ratio which would be measured by a lidar operating at 532 nm wavelength. Ice particles occur in an altitude range roughly between 80 and 92 km altitude. Typical number densities are $\sim$2000 cm^{-3} at 90 km and $\sim$100 cm^{-3} at 82 km consistent with current estimates of typical number densities responsible for PMSE and NLC, respectively. Mean radii on the other hand range between a few nanometer at 90 km and 30 nm at 82 km. The combination of these number densities and radii leads to a backscatter ratio peak of 5 at 82 km which is the altitude where NLCs are frequently observed. Note that this rather low value is due to our choice to average the data over one entire day. Maximum backscatter ratios calculated during the simulation are $\sim$ 75 and thus comparable to values experimentally observed.

3.2. Ice particles and PMSE

As outlined in section 2 the ice particles need to be charged in order to account for the reduction of electron diffusivity needed for the existence of PMSE.

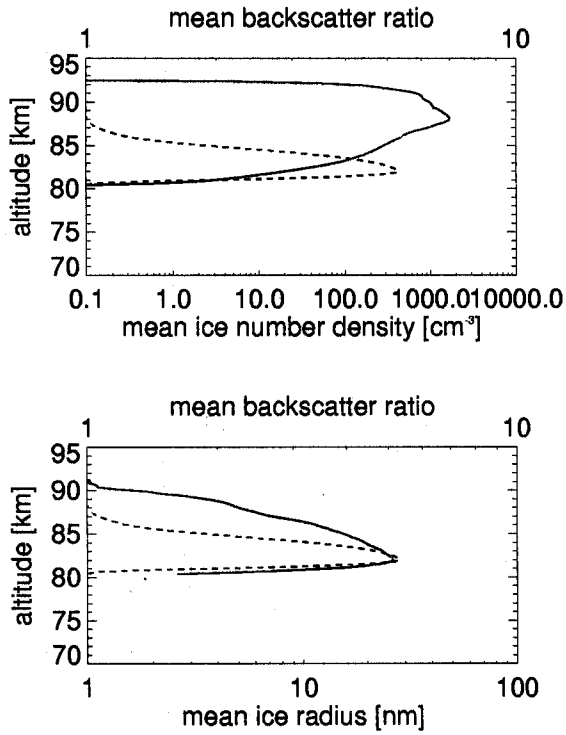

Figure 4. Ice number densities and mean radii (solid lines) averaged over the model simulation time of 1 day. The dashed line indicates the corresponding backscatter ratio which would be measured by a lidar operating at a wavelength of 532 nm.

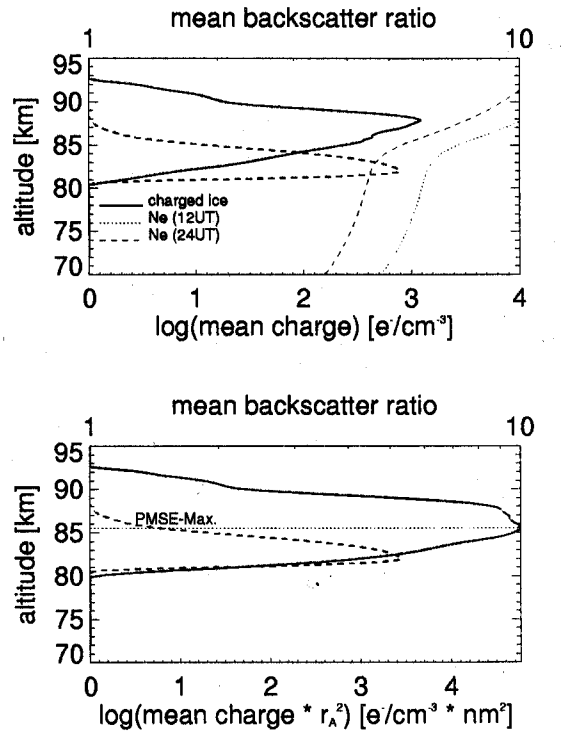

Figure 5. Charged aerosol number density (solid line) as estimated from model results obtained with the CARMA model and the average aerosol charge from Rapp and Lübken [2001]. The thin dashed and dotted lines to the left indicate standard electron density profiles obtained with the IRI model [Bilitza et al., 1993] and the thick dashed line indicates the backscatter ratio that would be observed by a lidar operating at 532 nm wavelength.

We thus estimate the charged aerosol number density from our model simulations using the average ice charge, Z_A, of an aerosol particle with a given radius from *Rapp and Lübken* [2001]. The results of this estimate are resented in the upper panel of Figure 5. Comparing the calculated aerosol charge number densities with a typical background electron density profile we note that the calculated values tend to be a bit too low to account for $\Lambda \geq 1$. However, the actual ice number density calculated with our model crucially depends on our assumption of the available amount of condensation nuclei. Lacking any better knowledge we use the meteoric smoke distribution from *Hunten et al.* [1980]. If we increase the amount of smoke particles say by a factor of ten, we also get more ice particles such that $\Lambda \geq 1$. This point could hint at the fact that the work of Hunten needs some reconsideration. This, however, is certainly beyond the scope of this article.

In order to include the r_A-dependence of the reduction of the electron mobility into our considerations we further present the height profile of the quantity $N_A Z_A \cdot r_A^2$ (see equation 12). This quantity shows a symmetric distribution around an altitude of 85 km which is the average altitude of PMSE [*Hoffmann et al.*, 1999]. Furthermore, we see that the mean backscatter ratio calculated from the model coincides with the lower edge of the $N_A Z_A \cdot r_A^2$-distribution. If we take the former quantity as a proxy for the possible existence of PMSE we thus find a nice agreement with common volume observations of lidars and radars which show that in the majority of cases the NLC is located at the lower edge of the PMSE [*von Zahn and Bremer*, 1999].

4. SUMMARY AND CONCLUSIONS

We have presented a model approach which explains the existence of electron density irregularities on spatial scales appropriate for the wavelengths of VHF radars. It has been shown that ambipolar electric fields due to the presence of charged aerosol particles efficiently suppress electron diffusivity provided that more than half of the electrons are bound to aerosol particles ($\Lambda \geq 1$). We have then used a microphysical model of the nucleation and growth of ice particles in the polar summer mesopause region and we have shown that the model is able to produce aerosol number densities and radii needed to account for both current NLC and PMSE observations. We find that the calculated altitude profile of

aerosol charge number density times the aerosol radius squared (the reduction of electron diffusivity is proportional to r_A^2) peaks at the altitude where the seasonal average maximum of PMSE occurs. This together with the fact that NLC backscatter ratios also calculated by the model yield the location of the NLC at the lower edge of this quantity is another strong indication that PMSE are indeed due to the ambipolar forces of negatively charged aerosols acting on the diffusivity of electrons.

However, the current investigation provides no answer to the question which process initially creates the irregularities in the electron densities. This point is currently under strong debate and will need additional experimental and theoretical efforts in the future to be understood.

ACKNOWLEDGEMENTS

We are grateful to E. J. Jensen and G. E. Thomas for providing the CARMA model.

REFERENCES

Belova, E., P. Chilson, M. Rapp, and S. Kirkwood, Electron temperature dependence of pmse power: experimental and modelling results, *Adv. Space Res., in print*, 2001.

Bilitza, D., K. Rawer, L. Bossy, and T. Gulyaeva, International reference ionosphere - past, present, future, *Adv. Space Res., 13*, 3–23, 1993.

Blix, T. A., and E. Thrane, Noctilucent clouds and regions with polar mesopheric summer echoes studied by means of rocket-borne electron and ion DC-probes, *Geophys. Res. Lett., 20*, 2303–2306, 1993.

Chilson, P. B., E. Belova, M. Rietveld, S. Kirkwood, and U.-P. Hoppe, First artificially induced modulation of pmse using the eiscat heating facility, *Geophys. Res. Lett., 27*, 3801–3804, 2000.

Cho, J. Y. N., T. M. Hall, and M. C. Kelley, On the role of charged aerosols in polar mesosphere summer echoes, *J. Geophys. Res., 97*, 875–886, 1992.

Czechowsky, P., R. Rüster, and G. Schmidt, Variations of mesospheric structures in different seasons, *Geophys. Res. Lett., 6*, 459–462, 1979.

Ecklund, W. L., and B. B. Balsley, Long-term observations of the arctic mesosphere with the MST radar at Poker Flat, Alaska, *J. Geophys. Res., 86*, 7775–7780, 1981.

Hervig, M., R. Thompson, M. McHugh, L. G. J. R. III, and M. Summers, First confirmation that water ice is the primary component of polar mesospheric clouds, *Geophys. Res. Lett., 28*, 971–974, 2001.

Hill, R. J., Nonneutral and quasi-neutral diffusion of weakly ionized multiconstituent plasma, *J. Geophys. Res., 83*, 989–998, 1978.

Hoffmann, P., W. Singer, and J. Bremer, Mean seasonal and diurnal variation of PMSE and winds from 4 years of radar observations at ALOMAR, *Geophys. Res. Lett., 26*, 1525–1528, 1999.

Hunten, D. M., R. P. Turco, and O. B. Toon, Smoke and dust particles of meteoric origin in the mesosphere and stratosphere, *J. Atmos. Sci., 37*, 1342–1357, 1980.

Jensen, E., and G. E. Thomas, A growth-sedimentation model of polar mesospheric clouds: Comparions with SME measurements, *J. Geophys. Res., 93*, 2461–2473, 1988.

Kelley, M. C., D. T. Farley, and J. Röttger, The effect of cluster ions on anomalous VHF backscatter from the summer polar mesosphere, *Geophys. Res. Lett., 14*, 1031–1034, 1987.

Kopp, E., P. Eberhardt, U. Herrmann, and L. Björn, Positive ion composition of the high latitude summer D-region with noctilucent clouds, *J. Geophys. Res., 90*, 13041–13051, 1985.

Körner, U., and G. Sonnemann, Global 3d-modelling of the water vapor concentration of the mesosphere/mesopause region and implications with respect to the nlc region, *J. Geophys. Res., in print*, 2001.

Lübken, F.-J., Thermal structure of the Arctic summer mesosphere, *J. Geophys. Res., 104*, 9135–9149, 1999.

Lübken, F.-J., M. Rapp, T. Blix, and E. Thrane, Microphysical and turbulent measurements of the Schmidt number in the vicinity of polar mesosphere summer echoes, *Geophys. Res. Lett., 25*, 893–896, 1998.

Rapp, M., and F.-J. Lübken, Electron temperature control of pmse, *Geophys. Res. Lett., 27*, 3285–3288, 2000.

Rapp, M., and F.-J. Lübken, Modelling of particle charging in the polar summer mesosphere: Part 1 – general results, *J. Atmos. Sol. Terr. Phys., 63*, 759–770, 2001.

Rapp, M., F.-J. Lübken, A. Müllemann, G. E. Thomas, and E. J. Jensen, Small scale temperature variations in the vicinity of NLC: Experimental and model results, *J. Geophys. Res., submitted*, 2001.

Turco, R. P., O. B. Toon, R. C. Whitten, R. G. Keesee, and D. Hollenbach, Noctilucent clouds: Simulation studies of their genesis, properties and global influences, *Planet. Space Sci., 3*, 1147–1181, 1982.

von Cossart, G., J. Fiedler, and U. von Zahn, Size distribution of NLC particles as determined from 3-color observations of NLC by ground based lidar, *Geophys. Res. Lett., 26*, 1513–1516, 1999.

von Zahn, U., and J. Bremer, Simultaneous and common-volume observations of noctilucent clouds and polar mesosphere summer echoes, *Geophys. Res. Lett., 26*, 1521–1524, 1999.